

Article

## A KAS-III Heterodimer in Lipstatin Biosynthesis Nondecarboxylatively Condenses C and C Fatty Acyl-CoA Substrates by a Variable Mechanism during the Establishment of a C Aliphatic Skeleton

Daozhong Zhang, Fang Zhang, and Wen Liu

*J. Am. Chem. Soc.*, **Just Accepted Manuscript** • DOI: 10.1021/jacs.8b12843 • Publication Date (Web): 14 Feb 2019

Downloaded from <http://pubs.acs.org> on February 14, 2019

### Just Accepted

“Just Accepted” manuscripts have been peer-reviewed and accepted for publication. They are posted online prior to technical editing, formatting for publication and author proofing. The American Chemical Society provides “Just Accepted” as a service to the research community to expedite the dissemination of scientific material as soon as possible after acceptance. “Just Accepted” manuscripts appear in full in PDF format accompanied by an HTML abstract. “Just Accepted” manuscripts have been fully peer reviewed, but should not be considered the official version of record. They are citable by the Digital Object Identifier (DOI®). “Just Accepted” is an optional service offered to authors. Therefore, the “Just Accepted” Web site may not include all articles that will be published in the journal. After a manuscript is technically edited and formatted, it will be removed from the “Just Accepted” Web site and published as an ASAP article. Note that technical editing may introduce minor changes to the manuscript text and/or graphics which could affect content, and all legal disclaimers and ethical guidelines that apply to the journal pertain. ACS cannot be held responsible for errors or consequences arising from the use of information contained in these “Just Accepted” manuscripts.

# A KAS-III Heterodimer in Lipstatin Biosynthesis Nondecarboxylatively Condenses C<sub>8</sub> and C<sub>14</sub> Fatty Acyl-CoA Substrates by a Variable Mechanism during the Establishment of a C<sub>22</sub> Aliphatic Skeleton

Daozhong Zhang<sup>1</sup>, Fang Zhang<sup>2</sup> and Wen Liu<sup>1,3,\*</sup>

<sup>1</sup> State Key Laboratory of Bioorganic and Natural Products Chemistry, Center for Excellence in Molecular Synthesis, Shanghai Institute of Organic Chemistry, University of Chinese Academy of Sciences, 345 Lingling Road, Shanghai 200032, China

<sup>2</sup> Innovation Research Institute of Traditional Chinese Medicine, Shanghai University of Traditional Chinese Medicine, 1200 Cailun Road, Shanghai 201203, China.

<sup>3</sup> Huzhou Center of Bio-Synthetic Innovation, 1366 Hongfeng Road, Huzhou 313000, China.

**ABSTRACT:**  $\beta$ -Ketoacyl-acyl carrier protein (ACP) synthase-III (KAS-III) and its homologs are thiolase-fold proteins that typically behave as homodimers functioning in diverse thioester-based reactions for C-C, C-O or C-N bond formation. Here, we report an exception observed in the biosynthesis of lipstatin. During the establishment of the C<sub>22</sub> aliphatic skeleton of this  $\beta$ -lactone lipase inhibitor, LstA and LstB, which both are KAS-III homologs but phylogenetically distinct from each other, function together by forming an unusual heterodimer to catalyze a nondecarboxylating Claisen condensation of C<sub>8</sub> and C<sub>14</sub> fatty acyl-CoA substrates. The resulting C<sub>22</sub>  $\alpha$ -alkyl  $\beta$ -ketoacid, which is unstable and tends to be spontaneously decarboxylated to a shunt C<sub>21</sub> hydrocarbon product, is transformed by the stereoselective  $\beta$ -ketoreductase LstD into a relatively stable C<sub>22</sub>  $\alpha$ -alkyl  $\beta$ -hydroxyacid for further transformation. LstAB activity tolerates changes in the stereochemistry, saturation degree and thioester form of both long-chain fatty acyl-CoA substrates. This flexibility, along with the characterization of catalytic residues, benefits our investigations into the individual roles of the two KAS-III homologs in the heterodimer-catalyzed reactions. The large subunit LstA contains a characteristic Cys-His-Asn triad, and likely reacts with C<sub>8</sub> acyl-CoA to form an acyl-Cys enzyme intermediate. In contrast, the small subunit LstB lacks this triad but possesses a catalytic Glu residue, which can act on the C<sub>8</sub> acyl-Cys enzyme intermediate in a substrate-dependent manner, either as a base for C $\alpha$  deprotonation or as a nucleophile for a Michael-type addition-initiated cascade reaction, to produce an enolate anion for head-to-head assembly with C<sub>14</sub> acyl-CoA through an unidirectional nucleophilic substitution. Uncovering LstAB catalysis draws attention to thiolase-fold proteins that are non-canonical in both active form and catalytic reaction/mechanism. LstAB Homologs are widespread in bacteria and remain to be functionally assigned, generating great interest in their corresponding products and associated biological functions.

## INTRODUCTION

$\beta$ -Ketoacyl-acyl carrier protein (ACP) synthase-III (KAS-III, e.g., FabH in *Escherichia coli*) catalyzes a decarboxylating Claisen condensation between acetyl-coenzyme A (CoA) and malonyl-ACP, yielding acetoacetyl-ACP (Figure 1A).<sup>1-3</sup> In plants and bacteria, this reaction initiates fatty acid biosynthesis and thus plays a role fundamentally important in cellular metabolism. KAS-III homologs (Figure S1), which share with the FabH archetype a highly conserved thiolase-fold and a characteristic Cys-His-Asn triad for catalysis, are widespread in plants, fungi and bacteria and involved in the biosynthesis of many bioactive secondary metabolites that hold promise for drug development. These homologs include the C-C bond-forming variants, such as Type III polyketide synthases

(PKSs) (Figure S1A),<sup>4-6</sup> which condense malonyl-CoA with variable acyl-CoA in a similar decarboxylative manner, and the C-O or C-N bond-forming variants (e.g., ChlB6, CerJ, PtmR, XclC and BomK), which essentially are acyltransferases and utilize thioester-based acyl donors for target molecule decoration (Figure S1B).<sup>7-11</sup> Recently, increasing evidence has indicated that KAS-III homologs (e.g., OleA, PpyS, StlD and DarB) catalyze nondecarboxylating condensations (Figure S1C), which in some cases can initiate a cyclization process in addition to the coupling of two acyl thioester units.<sup>12-15</sup> Despite functioning in diverse reactions, these proteins generally behave as homodimers during various catalytic processes. However, the KAS-III homologs in the biosynthesis of lipstatin represent an exception.

Lipstatin (Figure 1B), produced by *Streptomyces toxytricini*, is a naturally occurring lipase inhibitor.<sup>16,17</sup>

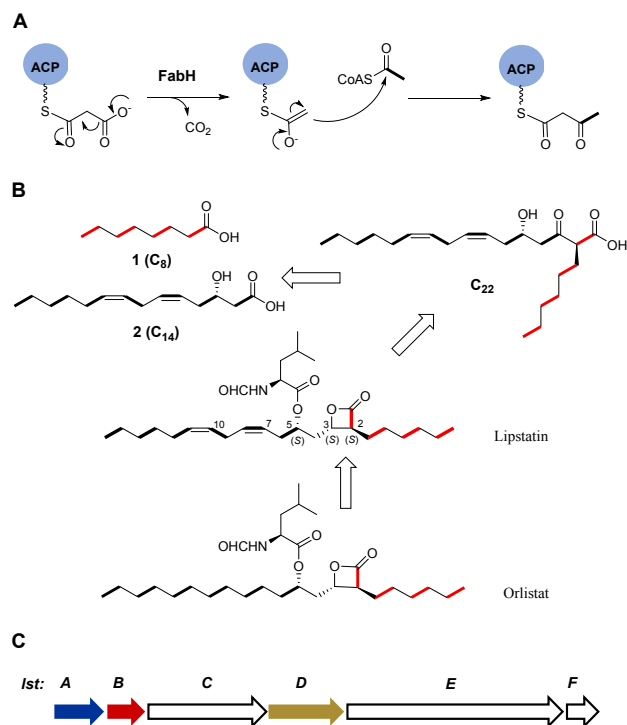


**Figure 1.** KAS-III and its homologs in the biosynthesis of lipstatin. **(A)** The canonical KAS-III FabH-catalyzed decarboxylating Claisen condensation for the initiation of fatty acid biosynthesis. **(B)** Retro-biosynthetic analysis of lipstatin and its derivative orlistat. The  $C_{22}$  aliphatic skeleton is labeled in bold and in color according to the  $C_8$  (red) and  $C_{14}$  (black) fatty acid precursors. The same below. **(C)** Biosynthetic genes of lipstatin. The genes in this study, i.e., *lstA* (blue) and *lstB* (red) coding for two distinct KAS-III homologs and *lstD* (yellow) for  $3\beta$ -HSD-eSDR-fold  $\beta$ -ketoreductase, are colored. The other genes include *lstC*, *lstE* and *lstF* that encode acyl-CoA synthetase, NRPS and formyltransferase, respectively.

It can be hydrogenated to orlistat (tetrahydrolipstatin, Figure 1B), a Food and Drug Administration-approved antiobesity agent that now forms the largest proportion of drugs consumed in obesity treatment.<sup>18</sup> The supply of orlistat depends primarily on the production of lipstatin by *S. toxytricini* fermentation; however, the process through which this precursor is biosynthesized remains poorly understood. Lipstatin features a highly strained  $\beta$ -lactone ring central to two aliphatic side chains that vary in length. In contrast to the short chain, which is saturated, the long chain is unsaturated and further functionalized with an *N*-formyl-leucine residue via an ester linkage. Isotope-labeling experiments have previously established that the  $C_{22}$   $\beta$ -lactone-containing olefinic skeleton of lipstatin arises from an unusual head-to-head assembly of octanoic acid (**1**,  $C_8$ ) and (3*S*,5*Z*,8*Z*)-3-hydroxytetradeca-5,8-dienoic acid (**2**,  $C_{14}$ ).<sup>19,20</sup> Both **1** and **2** can be derived from long-chain fatty acids through incomplete  $\beta$ -oxidation.<sup>21</sup> During this process, their CoA-based thioester forms (i.e., **1**-CoA and **2**-CoA) are produced, allowing for the occurrence of a Claisen condensation to afford an  $\alpha$ -alkyl  $\beta$ -ketoacid for  $\beta$ -

ketoreduction and subsequent  $\beta$ -lactonization. The biogenesis of lipstatin includes the genes coding for two KAS-III homologs, i.e., LstA (374-aa) and LstB (288-aa), which share 23% sequence identity with each other.<sup>22</sup> Both proteins are necessary for the biosynthesis of lipstatin, because inactivating the gene *lstA* or *lstB* in *S. toxytricini* exclusively abolished lipstatin production.<sup>22</sup> Notably, neither of the resulting mutant *S. toxytricini* strains produces condensed  $C_{22}$  intermediate(s). Starting with questioning whether LstA and LstB function together and participate in the unusual condensation of two long-chain ( $C_8$  and  $C_{14}$ ) fatty acyl-CoA substrates, we here focus on the *in vitro* reconstitution of the activities of these two distinct KAS-III homologs during the formation of the main carbon skeleton of lipstatin.

## RESULTS

**LstA and LstB form a heterodimer in solution.** To characterize the roles of LstA and LstB in the biosynthesis of lipstatin, we overexpressed their encoding genes in *E. coli*. Initially, our numerous attempts failed to prepare either of the KAS-III homologs in soluble form when expressing *lstA* or *lstB* alone. Within the *lst* operon (Figure 1C), these two genes are closely clustered for cotranscription. We thus cloned and coexpressed them both in *E. coli*, with the assumption that the resultant proteins can interact and cause a solubilization effect. Soluble protein complexes were observed when producing the two KAS-III homologs simultaneously (Figure S2A). Affinity purification was conducted on a Ni-NTA column by taking advantage of His-tag, which was fused either at the N-terminus of LstA or at the C-terminus of LstB. These complexes appeared to be single products under nondenaturing conditions, whereas under denaturing conditions, they decomposed exclusively into two distinct subunits with a ratio of  $\sim 1:1$  and the sizes appropriate to N-terminally 6 x His-tagged LstA ( $\sim 42.4$  kDa) and untagged LstB ( $\sim 29.3$  kDa) or untagged LstA ( $\sim 40.2$  kDa) and C-terminally 8 x His-tagged LstB ( $\sim 30.6$  kDa). Further analysis using multi-angle light scattering (MALS) indicated the heterodimerization state of these complexes (Figure S2B), with a molecular weight (MW) of  $\sim 68.0$  kDa. Clearly, LstA and LstB noncovalently interact with each other and form a heterodimer in solution.

**LstAB catalyzes nondecarboxylating condensations.** Using a complex composed of N-terminally 6 x His-tagged LstA and untagged LstB, we examined the condensation process *in vitro* to establish the main carbon skeleton of lipstatin. This process has long been speculated to occur in a decarboxylative manner (Figure S3).<sup>18</sup> The acyl-CoA carboxylase (ACCase) complex in *S. toxytricini* was suggested to catalyze the  $\alpha$ -carboxylation of **1**-CoA to hexylmalonyl (**3**)-CoA (Figure 2A). This  $C_9$  product might undergo  $\alpha$ -decarboxylation to form an enolate anion, which facilitates the reaction with **2**-CoA through nucleophilic substitution

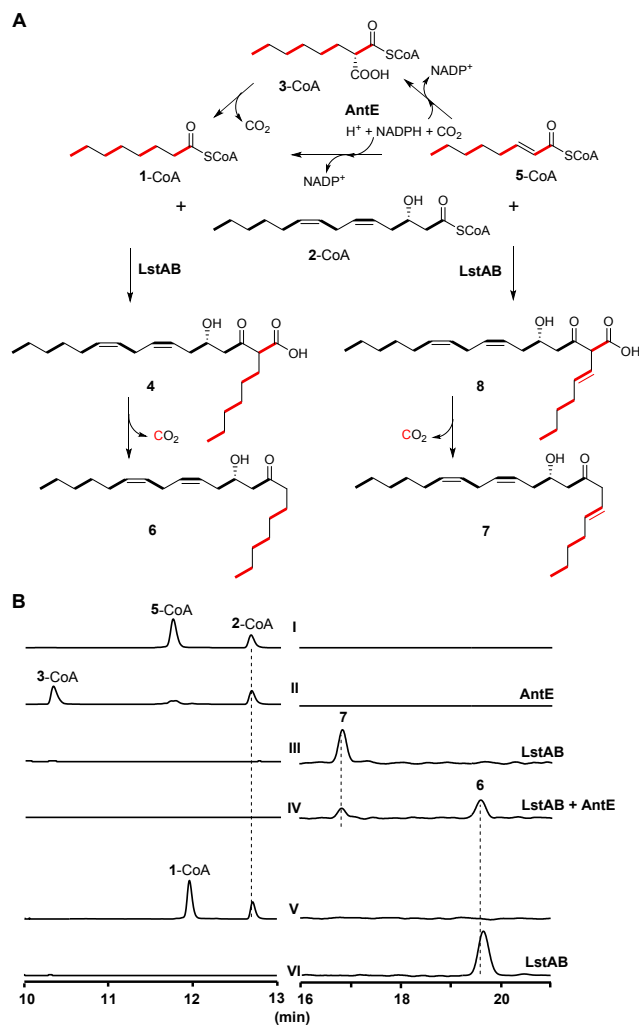


**Figure 2.** *In vitro* assays of the nondecarboxylating condensation activity of LstAB. (A) Transformations involving AntE and LstAB activities, respectively, for the preparation of  $\alpha$ -carboxylated 3-CoA and saturated 1-CoA from  $\alpha,\beta$ -unsaturated 5-CoA and the individual reactions of these C<sub>8</sub> acyl-CoA substrates with 2-CoA (C<sub>14</sub>) to produce C<sub>22</sub>  $\alpha$ -alkyl  $\beta$ -ketoacids (**4** and **8**) and shunt C<sub>21</sub> hydrocarbons (**6** and **7**). (B) HPLC analysis of substrate consumption and C<sub>21</sub> hydrocarbon production during LstAB catalysis over a 4-hr incubation period unless otherwise stated. For CoA-based products,  $\lambda$  at 245 nm; and for CoA-free products,  $\lambda$  at 210 nm. Using 5-CoA and 2-CoA, reactions were conducted in the absence of enzyme (I) and in the presence of AntE (II, 3 min), LstAB (III) and both AntE and LstAB (IV), respectively; and using 1-CoA and 2-CoA, reactions were performed in the absence (V) and presence (VI) of LstAB, respectively.

to yield a C<sub>22</sub>  $\alpha$ -branched  $\beta$ -ketoacid (**4**, (5*S*,7*Z*,10*Z*)-2-hexyl-5-hydroxy-3-oxohexadeca-7,10-dienoic acid, Figure 2A). Intriguingly, previous experimental evidence appeared to be contradictory. Consistent with this hypothesis that the  $\alpha$ -carboxylation of 1-CoA is necessary for condensation with 2-CoA, decomposing the ACCase complex *in vivo* by gene inactivation was supposed to negatively affect 3-CoA

preparation, and indeed, it led to an  $\sim 80\%$  decrease in lipstatin production and an  $\sim 4.5$ -fold increase in **2** accumulation.<sup>23</sup> However, inconsistency was found when isotope-labeled precursors were fed to *S. toxytricini*. Compared with **2**, **3** was incorporated into lipstatin at a relatively low rate, arguing that it does not serve as the direct condensing precursor.<sup>24</sup> Following the  $\alpha$ -decarboxylation-associated mechanism, we first synthesized 2-CoA and (2*E*)-octenyl (5)-CoA (Figures 2A and S4). After *in situ* transforming the  $\alpha,\beta$ -unsaturated precursor 5-CoA into the malonyl derivative 3-CoA using AntE (Figure 2A),<sup>25</sup> a highly flexible crotonyl-CoA reductase/carboxylase (CCR)-like protein that catalyzes reductive  $\alpha$ -carboxylation, we initiated reactions by adding the LstAB complex into the mixture (Figure 2B).

With LstAB, 2-CoA and newly produced 3-CoA in the reaction mixture were completely consumed over a 4-hr incubation period at 30°C. No CoA-based products were observed upon analysis by high-performance liquid chromatography (HPLC). Instead, we observed two CoA-free, hydrophobic small-molecule products, **6** and **7**, which differ from each other by 2 Da in MW. This reaction was scaled up, leading to the accumulation of sufficient products for structural elucidation by nuclear magnetic resonance (NMR) and high resolution mass spectrometry (HR-MS). Consequently, the major product, **6**, was characterized to be (1*S*,12*Z*,15*Z*)-10-hydroxyhenicosa-12,15-dien-8-one (Figure S12 and Table S3), a C<sub>21</sub> hydrocarbon assumedly arising from the decarboxylation of the resulting C<sub>22</sub>  $\alpha$ -branched  $\beta$ -ketoacid **4**, therefore validating the condensing activity of LstAB. Distinct from **6**, the minor C<sub>21</sub> hydrocarbon, **7** (Figure S13 and Table S4), is 5,6-unsaturated, and could be derived from the corresponding C<sub>22</sub> product, **8**, via decarboxylation. The finding of **7** production, which is unexpected (in both structure and producing mechanism, see Discussion), indicates that the reductive  $\alpha$ -carboxylation of 5-CoA to 3-CoA is unnecessary for condensation with 2-CoA. Consistently, **7** was observed in the reaction in which the CCR protein AntE was omitted, confirming that LstAB catalyzes the direct condensation of 5-CoA and 2-CoA. Inspired by these findings, we next simplified the above reaction mixture and assayed LstAB activity using 1-CoA and 2-CoA (Figure 2B). Remarkably, the condensation of these two precursors proceeded effectively, resulting in **6** as the sole detectable product by HPLC. Unambiguously, the LstAB complex constructs the main carbon skeleton of lipstatin in a nondecarboxylative manner, rather than in a decarboxylative manner as previously proposed. With regard to the production of **6** in the initial reaction mixture that contains AntE, we reasoned that either the spontaneous  $\alpha$ -decarboxylation of 3-CoA or the AntE-catalyzed side reaction for 5-CoA saturation can produce the direct precursor 1-CoA *in situ* for the following condensation with 2-CoA (Figure 2A).<sup>25</sup>

**Tracing the unstable C<sub>22</sub>  $\alpha$ -alkyl  $\beta$ -ketoacid.** During the condensation of 1-CoA and 2-CoA, we observed two putative C<sub>22</sub>  $\alpha$ -branched  $\beta$ -ketoacids (e.g., **4-I** and **4-II**) with the same MW in the HPLC-MS traces (Figure 3A). These condensed products, which are unstable because of

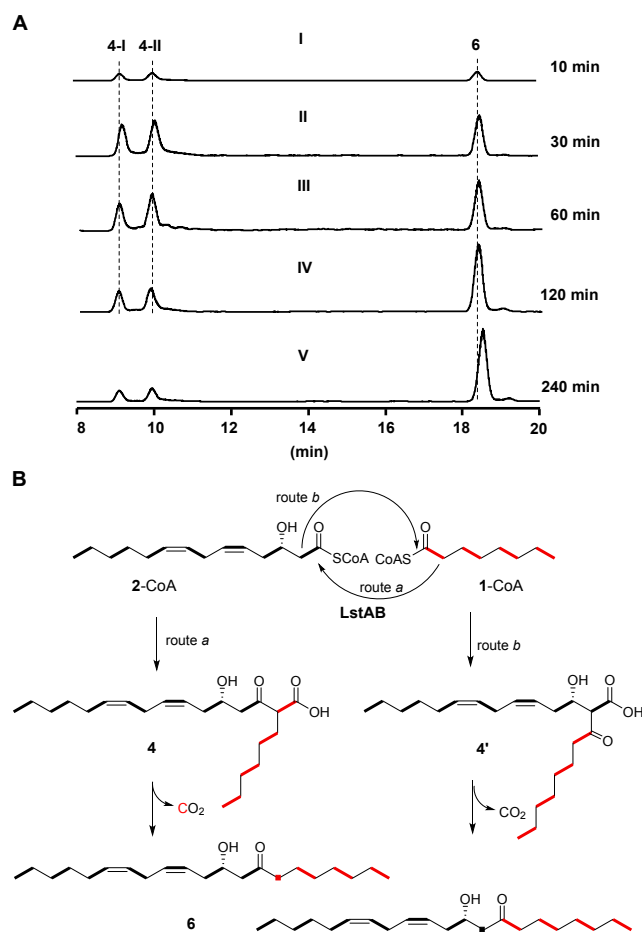


**Figure 3.** Characterization of the unstable  $C_{22}$   $\alpha$ -alkyl  $\beta$ -ketoacid in LstAB catalysis. (A) A time-course analysis of the LstAB-catalyzed condensation of **1-CoA** and **2-CoA** by HPLC-MS. ESI  $m/z$   $[M+H]^+$  for **4-I** and **4-II**, 367.0; and for **6**, 323.0. (B) Two possible routes for LstAB-catalyzed condensation to achieve the  $C_{21}$  hydrocarbons **6** after decarboxylation. Either **1-CoA** (route a, right) or **2-CoA** (route b, left) can be utilized as the nucleophilic substituent.

the low  $pK_a$  value of the  $\alpha$  hydrogen, reached maximum yields after 30 min and then decreased gradually with increase in the decarboxylated shunt  $C_{21}$  hydrocarbon (**6**). Mechanistically, the condensation of **1-CoA** with **2-CoA** can go through different nucleophilic substitutions to produce two possible  $C_{22}$   $\alpha$ -branched  $\beta$ -ketoacids, i.e., **4** and its isomer, **4'**, both of which could undergo decarboxylation to yield the same shunt  $C_{21}$  hydrocarbon **6** (Figure 3B). The route (b) in which **2** is the precursor subjected to  $\alpha$ -deprotonation for enolate anion formation is unlikely, because the structure of the product **4'** contrasts the  $C_{22}$  carbon skeleton of lipstatin (Figure 1B).<sup>19,20</sup> The two observed  $C_{22}$  products can be related to only **4**, which is generated through the route (a) utilizing **1** as the nucleophilic substituent (Figure 3B). Most likely, **4-I** and **4-II** represent the two isomeric forms of **4**, i.e., (2*S*)-**4** and (2*R*)-**4**, which can interconvert into each other rapidly in solution due to the active  $\alpha$  hydrogen that readily causes a proton exchange-coupled configuration change at C2.

Consistent with this conclusion, MS/MS analysis revealed that **4-I** and **4-II** were identical in fragmentation, and conducting this condensation reaction in  $D_2O$  led to the dominant production of the + 1 Da deuterium-labeled derivatives of both  $C_{22}$  products and the shunt  $C_{21}$  hydrocarbon **6** (Figure S5).

**LstD produces a relatively stable  $C_{22}$   $\alpha$ -alkyl  $\beta$ -hydroxyacid.** To support the notion that **4** is an intermediate in the biosynthesis of lipstatin, LstD, which shares sequence homology with members of the  $3\beta$ -hydroxysteroid dehydrogenase extended-short chain dehydrogenase/reductase ( $3\beta$ -HSD eSDR) superfamily,<sup>22</sup> was added into the above LstAB-involving reaction mixture for further transformation. This transformation led to the production of the + 2 Da reduced product **9**, with the disappearance of both **4-I** and **4-II** (Figure 4A). Spectral analyses revealed the identity of **9** to be (3*S*,5*S*,7*Z*,10*Z*)-2-hexyl-3,5-dihydroxyhexadeca-7,10-dienoic acid, a  $C_{22}$   $\alpha$ -alkyl  $\beta$ -hydroxyacid (Figure S14 and Table S5). Compared with **4**, **9** is relatively stable in solution because reducing  $\beta$ -keto to  $\beta$ -hydroxyl lowers the acidity at  $C\alpha$  and the decarboxylation tendency. These results confirmed the  $\beta$ -ketoreductase activity of LstD and supported the structural assignment for **4**. LstD could function stereoselectively and prefer (2*S*)-**4** as the substrate to drive the equilibrium with (2*R*)-**4** toward the production of **9** with an *S*-configuration at C3 (Figure 4B). During the purification process, **9** was found to be partially cyclized by lactonizing its carboxylate group with the hydroxyl group at C5, yielding **10**, a shunt 6-membered  $\delta$ -lactone product previously observed in mutant *S. toxytricini* strains that lack the ability of *N*-formyl-leucine incorporation (Figure S15).<sup>22</sup> During the biosynthesis of lipstatin, **9** may undergo a different intracellular lactonization with the C3 hydroxyl group to establish the aliphatic skeleton containing a more strained  $\beta$ -lactone, thereby leaving the C5 hydroxyl group for *N*-formyl-leucine functionalization.

**Identification of catalytic residues.** We aligned LstA and LstB sequences with selected FabH proteins and KAS-III homologs known to catalyze Claisen condensations (Figure S6). LstA shows overall head-to-tail homology with these proteins and contains a conserved triad composed of Cys128 $\alpha$ , His271 $\alpha$  and Asn305 $\alpha$ . In contrast, LstB has no such a triad and appears to be a much shortened KAS-III version that lacks the two particular sequences corresponding to those for the formation of the  $\beta 1$ - $\beta 2$ - $\alpha 3$ ,  $\eta 3$  and  $\alpha 8$  structures of the archetypal FabH.<sup>26</sup> We mutated the triad residues to Ala, and each engineered LstA protein was coproduced with LstB in *E. coli* (Figure S7). Intriguingly, the coproduction of LstA<sub>N305A</sub> with LstB failed to form a soluble heterodimer, suggesting that the residue Asn305 $\alpha$  is evolutionarily alienated from a catalytic role and instead plays a structural role in LstA or in its complex with LstB. Both complexes LstA<sub>C128A</sub>B and LstA<sub>H271A</sub>B were soluble and thus subjected to activity assays in the presence of **1-CoA** and **2-CoA** (Figure 4C).

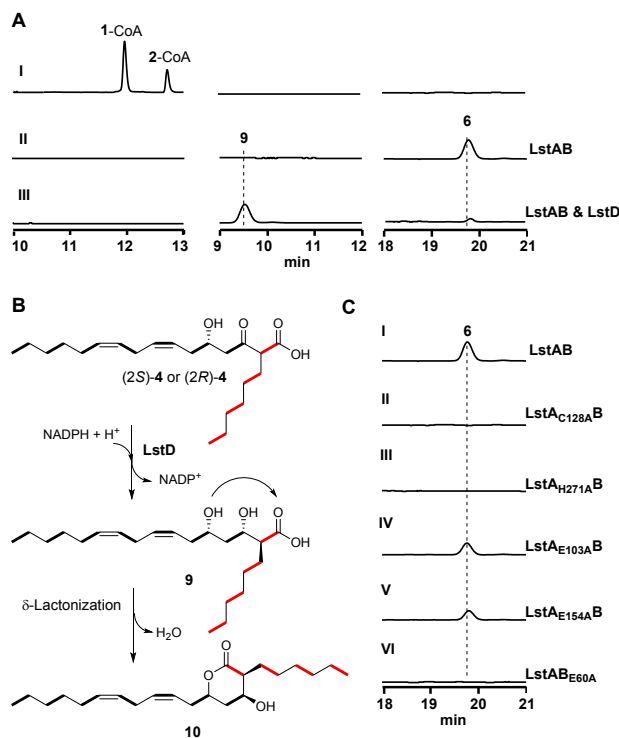


**Figure 4.** *In vitro* assays of the  $\beta$ -ketoreductase activity of LstD and the condensation activity of LstAB variants. For CoA-based products,  $\lambda$  at 245 nm; and for CoA-free products,  $\lambda$  at 210 nm. (A) HPLC analysis of substrate consumption and (shunt) product formation during LstD catalysis. Using 1-CoA and 2-CoA, reactions were conducted in the absence of enzyme (I) and in the presence of LstAB (II) and both LstAB and LstD (III), respectively. (B) LstD-catalyzed  $\beta$ -ketoreduction of 4 to the C<sub>22</sub>  $\alpha$ -alkyl  $\beta$ -hydroxyacid 9 and its cyclized derivative 10. (C) HPLC analysis of C<sub>21</sub> hydrocarbon production during the catalysis of each LstAB variant. I, wild-type LstAB; II, LstA<sub>C128A</sub>B; III, LstA<sub>H271A</sub>B; IV, LstA<sub>E103A</sub>B; V, LstA<sub>E154A</sub>B; and VI, LstA<sub>E60A</sub>B.

Neither LstA<sub>C128A</sub>B nor LstA<sub>H271A</sub>B produced the shunt C<sub>21</sub> hydrocarbon 6, validating the necessity of both Cys128 $\alpha$  and His271 $\alpha$  for LstAB catalysis. Most likely, Cys128 $\alpha$  is the residue responsible for covalently channeling an acyl group in the initial step of the condensation reaction. To exclude the possibility that LstB conducts this acyl carrier function, we mutated the residues that potentially act as a nucleophile in this shortened KAS-III homolog, including C33 $\beta$ , C98 $\beta$ , S21 $\beta$ , S42 $\beta$ , S88 $\beta$ , T58 $\beta$  and T245 $\beta$ . As anticipated, all of the corresponding heterodimers, i.e., LstA<sub>C33A</sub>B, LstA<sub>C98A</sub>B, LstA<sub>S21A</sub>B, LstA<sub>S42A</sub>B, LstA<sub>S88A</sub>B, LstA<sub>T58A</sub>B, and LstA<sub>T245A</sub>B, were soluble and exhibited condensation activity for 6 production (Figure S8).

The KAS-III homologs catalyzing nondecarboxylating condensations usually utilize a conserved Glu residue for  $\alpha$ -deprotonation/C $\alpha$  activation.<sup>14,27,28</sup> Accordingly, corresponding Glu residues in the LstAB complex (i.e., Glu103 $\alpha$  and Glu154 $\alpha$  in LstA and Glu60 $\beta$  in LstB) were identified and subjected to Ala-scanning, leading to the preparation of the soluble complexes LstA<sub>E103A</sub>B, LstA<sub>E154A</sub>B

and LstA<sub>E60A</sub>B for activity assays. Consequently, both LstA<sub>E103A</sub>B and LstA<sub>E154A</sub>B retained condensation activity, in contrast to LstA<sub>E60A</sub>B, which completely lost this ability and cannot condense 2-CoA with either 1-CoA or 5-CoA to produce 6 or 7, respectively (Figure 4C). Therefore, Glu60 $\beta$  is a residue necessary for LstAB activity, and the shortened KAS-III homolog LstB is a catalytic unit in addition to forming a complex with LstA.

**The flexibility of LstAB activity in substrate.** By examining the production of related shunt C<sub>21</sub> hydrocarbon products, we evaluated the substrate tolerance of the LstAB heterodimer. In terms of the short C<sub>8</sub> substrate, LstAB can utilize  $\alpha,\beta$ -unsaturated 5-CoA in the reaction with 2-CoA to produce 7 as mentioned above. Replacing 5-CoA with its isomer 5'-CoA, which is  $\beta,\gamma$ -unsaturated, also led to the production of 7 (Figure S4 and Figure S9). Focusing on the long C<sub>14</sub> substrate, we tested whether the commercially available (3S,5Z,8E)-3-hydroxytetradeca-5,8-dienoic acid (11) and 3-hydroxytetradecanoic acid (12) along with tetradecanoic acid (13), which was synthesized in this study, can be used as the precursors (Figure S4). These fatty acids were chemically transformed into their CoA derivatives, i.e., 11-CoA, 12-CoA and 13-CoA, which then individually reacted with 1-CoA in the presence of LstAB (Figure S9). Using 11-CoA led to the effective production of (3S,12Z,15E)-10-hydroxyhenicosa-12,15-dien-8-one, 14, which is a (15E)-stereoisomer of 6, indicating that LstAB activity is not sensitive to the stereochemistry of double bonds. Using 12-CoA resulted in 10-hydroxyhenicosan-8-one, 15, a condensed C<sub>21</sub> product that shares with orlistat a similar saturated main carbon skeleton. Therefore, saturation of the C<sub>14</sub> aliphatic chain have little effect. C<sub>21</sub> hydrocarbon failed to be produced when 13-CoA was used, confirming that the  $\beta$ -hydroxyl group of the C<sub>14</sub> acyl-CoA substrate is indispensable. In addition, both 2-CoA and 1-CoA can be replaced by their mimics of S-(N-acetyl) cysteamine (SNAC), i.e., 2-SNAC and 1-SNAC, and thiophenol (Sph), i.e., 2-Sph and 1-Sph, albeit with a lower yield in 6 production, indicating the changeability in the thioester forms of the fatty acyl substrates (Figures S4 and S9).

**Phylogenetic analysis.** In contrast to LstA, which is phylogenetically related to the KAS-III homologs OleA and PpyS that catalyze nondecarboxylating condensations and FabH proteins that function decarboxylatively for acetoacetyl-ACP formation, LstB appears to be relatively independently evolved and is distantly related to the clade of the KAS-III homologs that catalyze acyl transfer reactions for C-O or C-N bond formation (Figure 5A). Genome survey using *lstB* sequence revealed that *lstB* counterparts are widespread in various bacteria (Figure 5B), e.g., the species of *Streptomyces*, *Nocardia*, *Rhodococcus*, *Euyarchaeota* and *Mycobacterium*, leading to an interesting question concerning their intrinsic biological functions. In general, *lstB* counterparts are closely clustered with *lstA* counterparts, and in many cases, they both cluster with *lstD* counterparts.

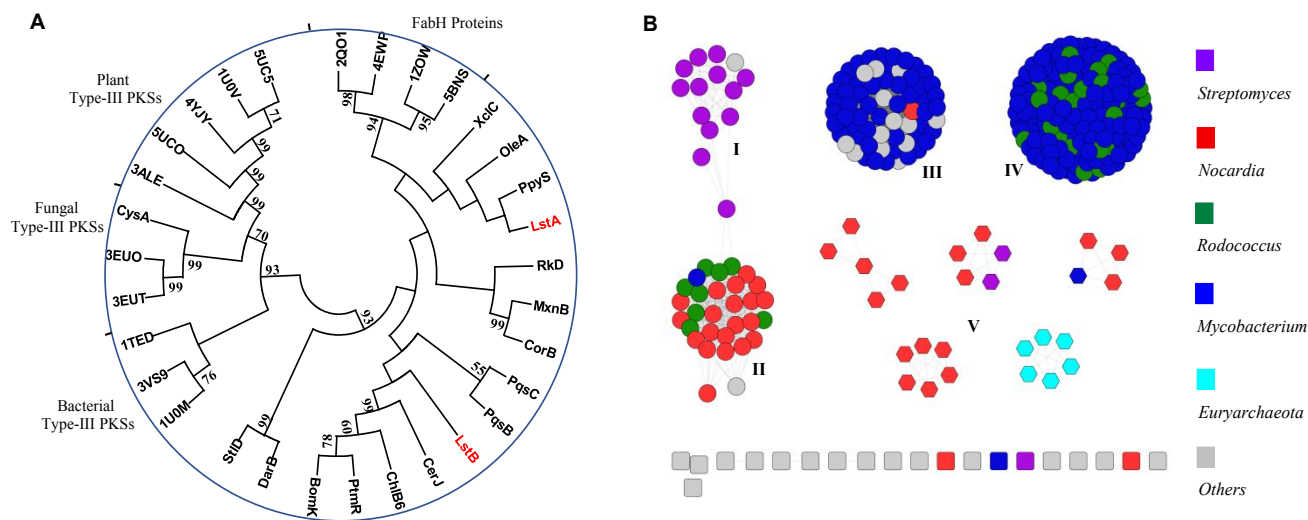


**Figure 5.** Phylogenetic analysis. **(A)** LstA and LstB (shown in red) with selected FabH proteins and KAS-III homologs (referred to Figure S1) in the phylogenetic tree. The evolutionary distances were computed using the Poisson correction method. **(B)** Sequence similarity networks of LstAB homologs (287) in bacteria. The chosen sequences share >25% identity with LstB. Members of Groups I, II and V (partial) are the LstAB homologs that are associated with LstD homologs. Bacterial species are indicated in color.

These findings indicate that in related bacteria, LstAB homologs might behave as heterodimers for long aliphatic chain assembly in a similar nondecarboxylative manner and particularly be involved in the formation of various  $\alpha$ -alkyl  $\beta$ -hydroxylacids with the association of LstD homologs (Figure S16A). Notably, mycolic acids, which are major lipid components of the cell envelope that are necessary for the survival of the genus *Mycobacterium* (including the causative agents of both tuberculosis and leprosy), are such long-chain  $\alpha$ -alkyl  $\beta$ -hydroxylacids.<sup>29-30</sup> Whether the reactions associated with LstAB and LstD activities complement the pathway known for mycolic acid biosynthesis in related *Mycobacterium* species as an alternative for  $\alpha$ -alkyl  $\beta$ -hydroxylacid supply remains to be determined. Some species share an entire *lst*-like cluster (*lstABCDEF*), implying that lipstatin-like  $\beta$ -lactones play an uncharacterized common biochemical role in addition to being recognized as a lipase inhibitor for human being (Figure S16B).

## DISCUSSION

KAS-III and its homologs belong to the thiolase superfamily, along with the condensing domains or components of KAS-I and KAS-II systems for aliphatic chain elongation in fatty acid biosynthesis and Type I and Type II PKS systems for polyketide biosynthesis, 3-hydroxy-3-methylglutaryl-CoA synthases involved in mevalonate-dependent isoprenoid biosynthesis and various thiolases catalyzing C-C bond formation or cleavage in both biosynthetic and degradative pathways.<sup>1-2</sup> Members of this superfamily share a common 3-dimensional fold but do not have to have recognizable sequence similarity. In Type II PKS systems, condensing activity comes from a complex composed of two different thiolase-fold proteins similar in

size, i.e., ketosynthase (KS) and chain length factor (CLF), which form a heterodimer capable of iteratively catalyzing decarboxylating Claisen condensation reactions.<sup>31</sup> While the KS component is responsible for polyketide chain assembly, the CLF component, which regulates polyketide chain length through an interaction with KS, does not have this synthetic ability. The other thiolase-fold proteins typically function as homodimers. Until this study, the only exception was recently observed in the biosynthesis of 2-heptyl-4(1*H*)-quinolone.<sup>32</sup> During the production of this *Pseudomonas aeruginosa* signal molecule, the KAS-III homologs PqsC (348-aa) and PqsB (283-aa) mimic the FabH homodimer by forming a heterodimer that possesses a pseudo-2-fold symmetry and catalyzes the decarboxylating condensation of octanoyl-CoA and 2-amino-benzoylacetate (2-ABA, a CoA-free  $\beta$ -keto acid).<sup>33</sup> Although LstA and LstB share moderate sequence homology to PqsC (19% identity) and PqsB (18% identity), respectively (Figure 5A), the two KAS-III homologs form a heterodimer differing from the PqsCB complex in the mechanism of carbon anion formation and the roles of subunits during catalytic process (Figure 6).

Given that no CoA-based products were observed, the large subunit LstA ( $\alpha$ ) was proposed to employ the triad residue Cys128 $\alpha$  as the nucleophile and react with the C<sub>8</sub> acyl-CoA substrate, forming a C<sub>8</sub> acyl-Cys128 $\alpha$  LstAB intermediate (although other mechanisms, e.g., the formation of a C<sub>14</sub> acyl-Cys128 $\alpha$  LstAB intermediate, cannot be excluded at this stage), and hydrolysis can follow the condensation of this enzyme intermediate with C<sub>14</sub> acyl-CoA substrate to produce a C<sub>22</sub>  $\alpha$ -alkyl  $\beta$ -ketoacid

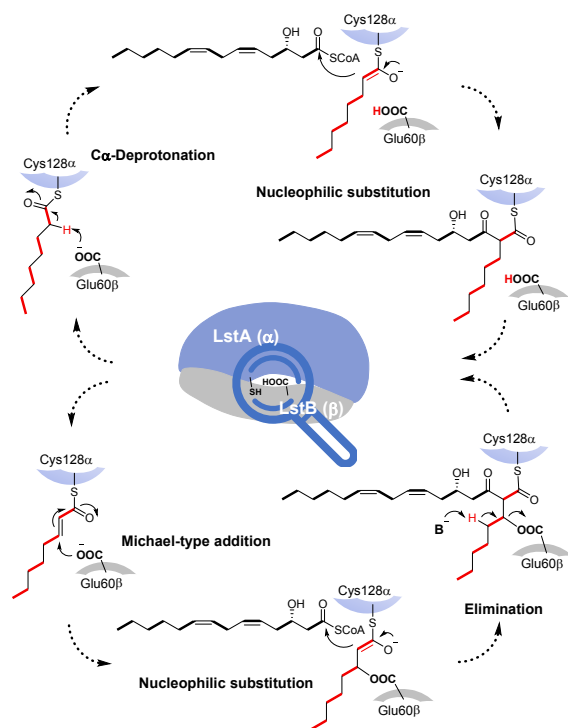


**Figure 6.** Proposed mechanisms of LstAB catalysis. Nondecarboxylating condensation can proceed in a substrate-dependent manner, either by  $\alpha$ -deprotonation (top) or by a Michael-type addition-initiated cascade reaction (bottom, in the case that  $\alpha,\beta$ -unsaturated substrate is used) to produce an enolate anion for an unidirectional nucleophilic substitution during the assembly of two long-chain fatty acyl-CoA substrates.

(Figure 6). While Asn305 $\alpha$  likely evolves to play a structural role, the triad residue His271 $\alpha$  is catalytically necessary. This residue, similar to its counterparts functioning in KAS-III homodimer-catalyzed non-decarboxylating reactions,<sup>33</sup> might be involved in acyl-enzyme formation or in an acylation-dependent increase in affinity for the second acyl-CoA substrate. Unlike PqsB, which essentially is a structural subunit in its complex with PqsC,<sup>33</sup> the small subunit LstB ( $\beta$ ) is a catalytic component in addition to forming a heterodimer with LstA. Sequence alignment revealed that Glu60 $\beta$  in LstB corresponds to the catalytic Glu residues of OleA and PpyS, the KAS-III homodimers catalyzing non-decarboxylating condensations (Figure S1), in line with the necessity of this residue for LstAB activity. Similarly, Glu60 $\beta$  may act as a base at the active site to deprotonate LstA-bound C<sub>8</sub> acyl at C $\alpha$  and form an enolate anion, thereby facilitating head-to-head assembly with C<sub>14</sub> acyl-CoA substrate (Figure 6). The LstAB-catalyzed condensation of 2-CoA with 1-CoA or  $\beta,\gamma$ -unsaturated 5'-CoA may share this mechanism, yielding the C<sub>22</sub>  $\alpha$ -alkyl  $\beta$ -ketoacid 4 or 8 and the corresponding shunt C<sub>21</sub> hydrocarbon 6 or 7.

Notably, the LstAB-catalyzed reaction of 2-CoA with 5-CoA cannot proceed by the above mechanism for enolate anion formation, because the C<sub>8</sub> acyl substrate is  $\alpha,\beta$ -

unsaturated and nonenolizable. The occurrence of this reaction had initially allowed us to consider C<sub>14</sub> acyl substrate being subjected to C $\alpha$  deprotonation. The fact that the nucleophilic substitution in LstAB catalysis is unidirectional excludes this possibility, otherwise the condensation would produce a distinct C<sub>22</sub>  $\alpha$ -alkyl  $\beta$ -ketoacid 8', which then undergoes decarboxylation to result in 7', a C<sub>21</sub> hydrocarbon different from the truly-observed shunt product 7 in double-bond position (Figure S10). We proposed that during the condensation of 2-CoA and 5-CoA, the catalytic residue Glu60 $\beta$  in LstB plays a distinct role by acting as a nucleophile. The addition of this nucleophile onto the (*Z*E)-octenyl-Cys128 $\alpha$  LstAB intermediate might lead to enolate anion formation through Michael-type addition (Figure 6B), which then can initiate an unusual cascade reaction, i.e., nucleophilic substitution and subsequent elimination, to produce the C<sub>22</sub> acyl-Cys128 $\alpha$  LstAB intermediate.

The functional characterization of LstAB as a unique KAS-III heterodimer, along with LstD as a 3 $\beta$ -HSD eSDR-fold  $\beta$ -ketoreductase, provides great insights into the biosynthesis of the  $\beta$ -lactone natural product lipstatin. In *S. toxytricini*, after hydrolysis and release from the LstAB heterodimeric complex, the highly labile C<sub>22</sub>  $\alpha$ -alkyl  $\beta$ -ketoacid intermediate 4, which tends to be spontaneously decarboxylated to the C<sub>21</sub> hydrocarbon 6, can be immediately reduced by LstD in a stereoselective manner, yielding the relative stable C<sub>22</sub>  $\alpha$ -alkyl  $\beta$ -hydroxyacid intermediate 9. This intermediate then undergoes  $\beta$ -lactonization, which could be catalyzed by the acyl-CoA synthetase-like protein LstC, and *N*-formyl-leucine substitution, which likely involves the both activities of the formyltransferase LstF and the nonribosomal peptide synthetase LstE, to achieve the structure underlying lipase inhibitor activity.

## CONCLUSION

In this study, we characterized the initial key steps for establishing the C<sub>22</sub> aliphatic skeleton of lipstatin in *S. toxytricini*. The two distinct KAS-III homologs LstA and LstB function together and form an unusual heterodimer to catalyze a nondecarboxylating Claisen condensation of two long-chain fatty acyl-CoA substrates, yielding a highly labile C<sub>22</sub>  $\alpha$ -alkyl  $\beta$ -ketoacid intermediate, which tends to be spontaneously decarboxylated to a C<sub>21</sub> hydrocarbon. This intermediate is reduced immediately by the 3 $\beta$ -HSD eSDR-fold protein LstD in a stereoselective manner, yielding a relatively stable C<sub>22</sub>  $\alpha$ -branched  $\beta$ -hydroxyacid intermediate for  $\beta$ -lactone formation and *N*-formyl-leucine substitution. LstAB activity is flexible and tolerates changes in stereochemistry, saturation degree and thioester form of both fatty acyl-CoA substrates. Uncovering LstAB catalysis adds attention to KAS-III homologs in the thiolase-fold superfamily, where to our knowledge, these proteins form the most diverse clade in both active form and catalytic reaction/mechanism. LstAB-like heterodimers are widespread in bacteria and remain to be functionally

assigned. Characterizing their products and associated biological functions would be extremely interesting.

## MATERIALS AND METHODS

**Sequence analysis.** Target proteins were compared with other known proteins in the databases using available BLAST methods (<http://blast.ncbi.nlm.nih.gov/Blast.cgi>). Sequence alignments were performed using Vector NT1 and ESPript 3.0 (<http://esprript.ibcp.fr/ESPript/ESPript/>). Sequence similarity networks were generated using the EFI-EST webtool (<http://efi.igb.illinois.edu/efi-est/>).

**Site-specific mutagenesis.** Rolling-cycle PCR amplification of (using the primers listed in Table S2) followed by subsequent DpnI digestion was conducted to produce the genes coding for LstA or LstB variants, according to the standard procedure of the QuikChange Site-Directed Mutagenesis Kit purchased from Stratagene (USA) or Mut Express II (Vazyme Biotech Co. Ltd, China). Each mutation was confirmed by sequencing.

**Assays of LstAB activity.** Initial assays that follow the decarboxylating mechanism for enolate anion formation were carried out over a 4-hr incubation period at 30°C each in a 100  $\mu$ L reaction mixture containing 100 mM Tris-HCl (pH 7.5), 5 mM reduced form of nicotinamide-adenine dinucleotide phosphate (NADPH), 2 mM MgCl<sub>2</sub>, 1 mM trichloroethyl phosphate (TCEP), 30 mM NaHCO<sub>3</sub>, and 1 mM 5-CoA and 1 mM 2-CoA. 5  $\mu$ M AntE was added into the reaction mixture, and the *in situ* transformation of 5-CoA to  $\alpha$ -carboxylated 3-CoA was nearly completed after 3 min at 30°C (for details in determining the conditions of AntE-catalyzed reductive  $\alpha$ -carboxylation, see *SI Materials and Methods*). 10  $\mu$ M LstAB was then incorporated to initiate the condensation process. The reactions in which AntE, LstAB or both were omitted were used as the controls.

The assays that follow the nondecarboxylating mechanism for enolate anion formation were carried out at 30°C each in a 100  $\mu$ L reaction mixture containing 100 mM Tris-HCl (pH 7.5), 2 mM MgCl<sub>2</sub>, 1 mM TCEP, 1 mM 1-CoA and 1 mM 2-CoA. 10  $\mu$ M LstAB was added into the reaction mixture to initiate the condensation process. The reaction conducted in the absence of LstAB was used as the control. For a time-course analysis of (shunt) product formation, the reactions were performed at 30°C for 10 min, 30 min, 60 min, 120 min and 240 min, respectively.

For examining the proton exchange of the C<sub>22</sub>  $\alpha$ -alkyl  $\beta$ -ketoacid 4, assays were carried out at 30°C for 30 min in a D<sub>2</sub>O-complemented reaction mixture containing 100 mM Tris-HCl (pH 7.5), 2 mM MgCl<sub>2</sub>, 1 mM TCEP, 1 mM 1-CoA, 1 mM 2-CoA and 10  $\mu$ M LstAB.

**Assays of LstD activity.** To prepare the C<sub>22</sub>  $\alpha$ -alkyl  $\beta$ -ketoacid substrate *in situ*, assays were carried out at 30°C each in a 100  $\mu$ L reaction mixture containing 100 mM Tris-HCl (pH 7.5), 2 mM MgCl<sub>2</sub>, 1 mM TCEP, 1 mM 1-CoA, 1 mM 2-CoA and 10  $\mu$ M LstAB. After incubation for 30 min, 5 mM NADPH and 5  $\mu$ M LstD were added into the reaction mixture before further incubation at 30°C for 2 hr. The reactions in which LstD or both LstD and LstAB were omitted were used as the controls.

**Product examination.** For CoA-based products, related reactions were quenched by addition of 1% TCA (*v/v*). After centrifugation at 12,000 rpm for 5 min, the supernatant was subjected to HPLC or HPLC-ESI-MS analysis on an Agilent Zorbax column (SB-C18, 5  $\mu$ m, 4.6 x 250 mm, Agilent Technologies Inc., USA) by gradient elution of solvent A (5 mM NH<sub>4</sub>OAc) and solvent B (CH<sub>3</sub>CN) at a flow rate of 1 mL min<sup>-1</sup> over a 30-min period as follows: *t* = 0-5 min, 5% B; *t* = 5-25 min, 5%-100% B; and *t* = 25-30 min, 100% B ( $\lambda$  at 245 nm).

For CoA-free products, each reaction (100  $\mu$ L) was quenched using an equal volume of CH<sub>3</sub>CN. After freeze-drying, residues were dissolved in 60  $\mu$ L of CH<sub>3</sub>CN and then subjected to HPLC or HPLC-ESI-MS analysis on the same column by gradient elution of solvent A (water containing 0.1% formic acid) and solvent B (CH<sub>3</sub>CN containing 0.1% formic acid) at a flow rate of 1 mL min<sup>-1</sup> over a 30-min period as follows: *t* = 0-10 min, 80% B; *t* = 11-20 min, 90% B; and *t* = 21-30 min, 100% B ( $\lambda$  at 210 nm).

**Scale-up for product preparation.** The C<sub>21</sub> hydrocarbon 6 was produced in a 10 mL reaction mixture containing 100 mM Tris-HCl (pH 7.5), 5 mM NADPH, 2 mM MgCl<sub>2</sub>, 1 mM TCEP, 30 mM NaHCO<sub>3</sub>, and 1 mM 5-CoA, 1 mM 2-CoA, 5  $\mu$ M AntE and 10  $\mu$ M LstAB. The C<sub>21</sub> hydrocarbon 7 was prepared in an 80 mL reaction mixture containing 100 mM Tris-HCl (pH 7.5), 2 mM MgCl<sub>2</sub>, 1 mM TCEP, 10% DMSO, 1 mM 2-CoA, 2 mM 5-CoA and 100  $\mu$ M LstAB. The C<sub>22</sub>  $\alpha$ -alkyl  $\beta$ -hydroxyacid 9 was produced in a 20 mL reaction mixture containing 100 mM Tris-HCl (pH 7.5), 2 mM MgCl<sub>2</sub>, 1 mM TCEP, 10% DMSO, 1 mM 1-SNAC, 2 mM 2-SNAC, 5 mM NADPH, 100  $\mu$ M LstAB and 10  $\mu$ M LstD. Reaction mixtures were incubated at 30°C overnight and then quenched by adding an equal volume of CH<sub>3</sub>CN. After centrifugation at 12,000 for 10 min, supernatants were lyophilized overnight. Residues were dissolved in 5 mL of CH<sub>3</sub>CN, followed by semi-preparative HPLC on an Agilent Zorbax column (SB-C18, 5  $\mu$ m, 9.4 x 250 mm, Agilent Technologies Inc., USA) under the conditions described above. Purified product were dissolved in the CDCl<sub>3</sub> for NMR analysis (in CDCl<sub>3</sub>, Tables S3-5). Compound 6, HR-ESI-MS *m/z* for C<sub>21</sub>H<sub>39</sub>O<sub>2</sub><sup>+</sup>: calcd. [M+H]<sup>+</sup> = 323.2945, found 323.2946; compound 7, HR-ESI-MS *m/z* for C<sub>21</sub>H<sub>37</sub>O<sub>2</sub><sup>+</sup>: calcd. [M+H]<sup>+</sup> = 321.2788, found 321.2795; and compound 9, HR-ESI-MS *m/z* for C<sub>21</sub>H<sub>38</sub>O<sub>2</sub>Na<sup>+</sup>: calcd. [M+Na]<sup>+</sup> = 391.2819, found 391.2824.

## ASSOCIATED CONTENT

### Supporting Information

The Supporting Information is available free of charge on the ACS Publications website at DOI: xxxxx.

Supplementary materials and methods (i.e., general materials and methods, protein expression and purification, chemical synthesis and compound characterization), results, Figures S1-S14, and Tables S1-S6.

## AUTHOR INFORMATION

Corresponding Author

\*[wliu@sioc.ac.cn](mailto:wliu@sioc.ac.cn)

## Funding Sources

This work was supported in part by grants from NSFC (21750004, 31430005, 21520102004, 21472231 and 21621002), CAS (QYZDJ-SSW-SLH037 and XDB20020200), STCSM (17JC1405100), MST (2018ZX091711001-006-010) and K. C. Wang Education Foundation.

## Notes

The authors declare no competing financial interest.

## ACKNOWLEDGMENT

The authors thank Yanping Qiu and Heng Guo for collecting NMR and HR-MS data. The authors show our gratitude to Zhi Lin and Zhijun Tang for reviewing manuscript and other people in our lab for their practical support.

## ABBREVIATIONS

CCR2, CC chemokine receptor 2; CCL2, CC chemokine ligand 2; CCR5, CC chemokine receptor 5; TLC, thin layer chromatography.

## REFERENCES

1. Heath, R. J.; Rock, C. O., The Claisen condensation in biology. *Nat. Prod. Rep.* **2002**, *19*, 581-596.
2. Haapalainen, A. M.; Merilainen, G.; Wierenga, R. K., The thiolase superfamily: condensing enzymes with diverse reaction specificities. *Trends Biochem. Sci.* **2006**, *31*, 64-71.
3. Zhang, H.; Machutta, C. A.; Tonge, P. J., Fatty Acid Biosynthesis and Oxidation. In *Comprehensive Natural Products II*, Liu, H.-W.; Mander, L., Eds. Elsevier: Oxford, 2010; Vol. 8, pp 231-275.
4. Sukovich, D. J.; Seffernick, J. L.; Richman, J. E.; Hunt, K. A.; Gralnick, J. A.; Wackett, L. P., Structure, function, and insights into the biosynthesis of a head-to-head hydrocarbon in *Shewanella oneidensis* strain MR-1. *Appl. Environ. Microbiol.* **2010**, *76*, 3842-9.
5. Hashimoto, M.; Nonaka, T.; Fujii, I., Fungal type III polyketide synthases. *Nat. Prod. Rep.* **2014**, *31*, 1306-17.
6. Shimizu, Y.; Ogata, H.; Goto, S., Type III polyketide synthases: functional classification and phylogenomics. *ChemBioChem* **2017**, *18*, 50-65.
7. He, Q.-L.; Jia, X.-Y.; Tang, M.-C.; Tian, Z.-H.; Tang, G.-L.; Liu, W., Dissection of two acyl-transfer reactions centered on acyl-carrier protein intermediates for incorporating 5-chloro-6-methyl-o-methylsalicylic acid into chlorothricin. *ChemBioChem* **2009**, *10*, 813-819.
8. Bretschneider, T.; Zocher, G.; Unger, M.; Scherlach, K.; Stehle, T.; Hertweck, C., A ketosynthase homolog uses malonyl units to form esters in cervimycin biosynthesis. *Nat. Chem. Biol.* **2012**, *8*, 154-161.
9. Lv, M.; Zhao, J.; Deng, Z.; Yu, Y., Characterization of the biosynthetic gene cluster for benzoxazole antibiotics A33853 reveals unusual assembly logic. *Chem. Biol.* **2015**, *22*, 1313-1324.
10. Abugrain, M. E.; Brumsted, C. J.; Osborn, A. R.; Philmus, B.; Mahmud, T., A Highly Promiscuous  $\beta$ -Ketoacyl-ACP Synthase (KAS) III-like protein is involved in pactamycin biosynthesis. *ACS Chem. Biol.* **2017**, *12*, 362-366.
11. Proschak, A.; Zhou, Q.; Schöner, T.; Thanwisai, A.; Kresovic, D.; Dowling, A.; ffrench-Constant, R.; Proschak, E.; Bode, H. B., Biosynthesis of the Insecticidal Xenoclyoins in *Xenorhabdus bovienii*. *ChemBioChem* **2014**, *15*, 369-372.
12. Frias, J. A.; Richman, J. E.; Erickson, J. S.; Wackett, L. P., Purification and characterization of OleA from *Xanthomonas campestris* and demonstration of a non-decarboxylative Claisen condensation reaction. *J. Biol. Chem.* **2011**, *286*, 10930-8.
13. Brachmann, A. O.; Brameyer, S.; Kresovic, D.; Hitkova, I.; Kopp, Y.; Manske, C.; Schubert, K.; Bode, H. B.; Heermann, R., Pyrones as bacterial signaling molecules. *Nat. Chem. Biol.* **2013**, *9*, 573-578.
14. Mori, T.; Awakawa, T.; Shimomura, K.; Saito, Y.; Yang, D.; Morita, H.; Abe, I., Structural insight into the enzymatic formation of bacterial stilbene. *Cell Chem. Biol.* **2016**, *23*, 1468-1479.
15. Fuchs, S. W.; Bozhuyuk, K. A.; Kresovic, D.; Grundmann, F.; Dill, V.; Brachmann, A. O.; Waterfield, N. R.; Bode, H. B., Formation of 1,3-cyclohexanediones and resorcinols catalyzed by a widely occurring ketosynthase. *Angew. Chem. Int. Ed. Engl.* **2013**, *52*, 4108-4112.
16. Weibel EK, H. P., Hochuli E, Kupfer E, Lengsfeld H, Lipstatin, an inhibitor of pancreatic lipase, produced by *Streptomyces toxytricini*. I. Producing organism, fermentation, isolation and biological activity. *J. Antibiot. (Tokyo)* **1987**, *40*, 1081-1085.
17. Hochuli, E.; Kupfer, E.; Maurer, R.; Meister, W.; Mercadal, Y.; Schmidt, K., Lipstatin, an inhibitor of pancreatic lipase, produced by *Streptomyces toxytricini*. II. Chemistry and structure elucidation. *J. Antibiot (Tokyo)* **1987**, *40*, 1086-1091.
18. Kumar, P.; Dubey, K. K., Current trends and future prospects of lipstatin: a lipase inhibitor and pro-drug for obesity. *RSC Advances* **2015**, *5*, 86954-86966.
19. Eisenreich, W.; Kupfer, E.; Weber, W.; Bacher, A., Tracer studies with crude U-<sup>13</sup>C-lipid mixtures: biosynthesis of the lipase inhibitor lipstatin. *J. Biol. Chem.* **1997**, *272*, 867-874.
20. Goese, M.; Eisenreich, W.; Kupfer, E.; Stohler, P.; Weber, W.; Leuenberger, H. G.; Bacher, A., Biosynthesis of Lipstatin. Incorporation of multiply deuterium-labeled (5Z,8Z)-tetradeca-5,8-dienoic acid and octanoic acid. *J. Org. Chem.* **2001**, *66*, 4673-4678.
21. Goese, M.; Eisenreich, W.; Kupfer, E.; Weber, W.; Bacher, A., Biosynthetic origin of hydrogen atoms in the lipase inhibitor lipstatin. *J. Biol. Chem.* **2000**, *275*, 21192-21196.
22. Bai, T.; Zhang, D.; Lin, S.; Long, Q.; Wang, Y.; Ou, H.; Kang, Q.; Deng, Z.; Liu, W.; Tao, M., Operon for biosynthesis of lipstatin, the beta-lactone inhibitor of human pancreatic lipase. *Appl. Environ. Microbiol.* **2014**, *80*, 7473-7483.
23. Demirev, A. V.; Khanal, A.; Sedai, B. R.; Lim, S. K.; Na, M. K.; Nam, D. H., The role of acyl-coenzyme A carboxylase complex in lipstatin biosynthesis of *Streptomyces toxytricini*. *Appl. Microbiol. Biotechnol.* **2010**, *87*, 1129-1139.
24. Schuhr, C. A.; Eisenreich, W.; Goese, M.; Stohler, P.; Weber, W.; Kupfer, E.; Bacher, A., Biosynthetic precursors of the lipase inhibitor lipstatin. *J. Org. Chem.* **2002**, *67*, 2257-2262.
25. Yan, Y.; Chen, J.; Zhang, L.; Zheng, Q.; Han, Y.; Zhang, H.; Zhang, D.; Awakawa, T.; Abe, I.; Liu, W., Multiplexing of combinatorial chemistry in antimycin biosynthesis: expansion of molecular diversity and utility. *Angew. Chem. Int. Ed.* **2013**, *52*, 12308-12312.
26. White, S. W.; Zheng, J.; Zhang, Y.-M.; Rock, C. O., the structural biology of type II fatty acid biosynthesis. *Annu. Rev. Biochem* **2005**, *74*, 791-831.
27. Goblirsch, B. R.; Jensen, M. R.; Mohamed, F. A.; Wackett, L. P.; Wilmot, C. M., Substrate trapping in crystals of the thiolase OleA identifies three channels that enable long chain olefin biosynthesis. *J. Biol. Chem.* **2016**, *291*, 26698-26706.
28. Kresovic, D.; Schempp, F.; Cheikh-Ali, Z.; Bode, H. B., A novel and widespread class of ketosynthase is responsible for the head-to-head condensation of two acyl moieties in bacterial pyrone biosynthesis. *Beilstein J. Org. Chem.* **2015**, *11*, 1412-1417.
29. Marrakchi, H.; Lanéelle, M.-A.; Daffé, M., Mycolic acids: structures, biosynthesis, and beyond. *Chem. Biol.* **2014**, *21*, 67-85.

1 30. Quémard, A., New insights into the mycolate-containing  
2 compound biosynthesis and transport in mycobacteria. *Trends*  
3 *Microbiol.* **2016**, *24*, 725-738.

4 31. Keatinge-Clay, A. T.; Maltby, D. A.; Medzihradzky, K. F.;  
5 Khosla, C.; Stroud, R. M., An antibiotic factory caught in action. *Nat.*  
6 *Struct. Mol. Biol.* **2004**, *11*, 888-93.

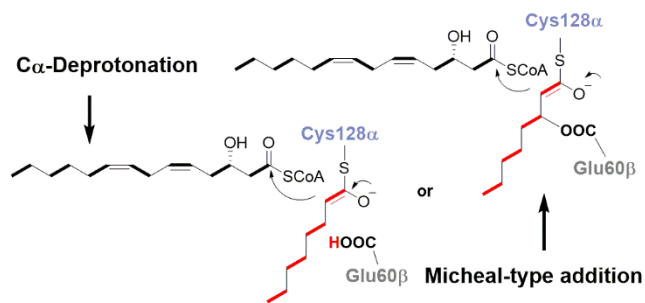
7 32. Dulcey, Carlos E.; Dekimpe, V.; Fauvelle, D.-A.; Milot, S.;  
8 Groleau, M.-C.; Doucet, N.; Rahme, Laurence G.; Lépine, F.; Déziel,  
9 E., The End of an Old Hypothesis: The *Pseudomonas* signaling

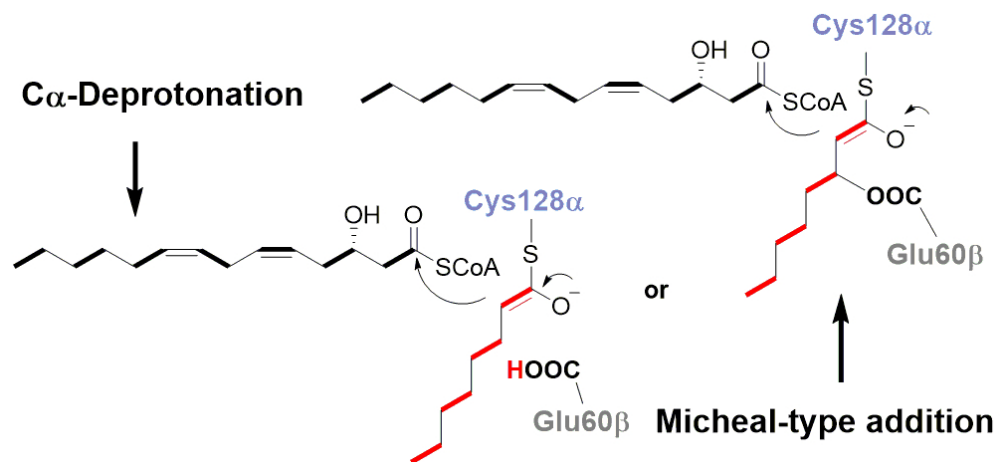
molecules 4-hydroxy-2-alkylquinolines derive from fatty acids, not  
3-ketofatty acids. *Chem. Biol.* **2013**, *20*, 1481-1491.

33. Drees, S. L.; Li, C.; Prasetya, F.; Saleem, M.; Dreveny, I.;  
Williams, P.; Hennecke, U.; Emsley, J.; Fetzner, S., PqsBC, a  
condensing enzyme in the biosynthesis of the pseudomonas  
aeruginosa quinolone signal: crystal structure, inhibition, and  
reaction mechanism. *J. Biol. Chem.* **2016**, *291*, 6610-6624.

1  
2  
3  
4  
5  
6  
7  
8  
9  
10  
11  
12  
13  
14  
15  
16  
17  
18  
19  
20  
21  
22  
23  
24  
25  
26  
27  
28  
29  
30  
31  
32  
33  
34  
35  
36  
37  
38  
39  
40  
41  
42  
43  
44  
45  
46  
47  
48  
49  
50  
51  
52  
53  
54  
55  
56  
57  
58  
59  
60

Insert Table of Contents artwork here





85x40mm (300 x 300 DPI)